Journal of Applied Polymer Science

In situ polymerization of polyurethane-silver nanocomposite foams with intact thermal stability, improved mechanical performance, and induced antimicrobial properties

Tarek M. Madkour,[1] Eman A. Abdelazeem,[1*] Amr Tayel,[1] Ghada Mustafa,[2,3] Rania Siam[2,3]

[1]Department of Chemistry, The American University in Cairo, AUC Avenue, P.O. Box 74, New Cairo 11835, Egypt

[2]Biology Department, The American University in Cairo, AUC Avenue, P.O. Box 74, New Cairo 11835, Egypt

[3]Yousef Jameel Science & Technology Research Center (YJ-STRC), The American University in Cairo, AUC Avenue, P.O. Box 74, New Cairo 11835, Egypt

*The work described in this article is based in part on the graduation senior thesis of the second author.

Correspondence to: T. M. Madkour (E-mail: tarekmadkour@aucegypt.edu)

ABSTRACT: Silver nanoparticle-reinforced thermoplastic polyurethane (PU/AgNP) nanocomposite foams were prepared using *in situ* polymerization techniques in accordance with DOW chemicals' industrial standards. The foams exhibited improved mechanical performance, induced antimicrobial properties, and intact stability when subjected to a thermal degradation treatment. Scanning electron microscopy (SEM) indicated a homogeneous dispersion of the silver nanoparticle (AgNP) within the polymeric matrix at low filler loadings and a cluster formation at higher loadings. SEM also indicated the agglomeration of the silver nanofiller particles as a result of the thermal degradation treatment, which caused them to lose their nanoscopic characteristics and act as ordinary silver metal. Molecular modeling techniques were used to explain these observations and confirmed the higher repulsive interactions between the polymer chains and the silver nanoparticles with the increase in the nanofiller content. Stress relaxation of the nanocomposites showed optimum mechanical performance and lowest hysteresis for the 0.1% AgNP nanocomposites due to the confinement of the PU chains between the large number of the nanoparticles. Incubation with 0.1% foam inhibited the growth of *Klebseilla* spp. and *Escherichia coli* and to some extent *Staphylococcus* spp. This is very interesting as the same nanocomposite loaded with 0.1% AgNp has also shown the best mechanical performance highlighting the strong action of this "unclustered" low concentration on both the material and biomedical sides. © 2015 Wiley Periodicals, Inc. J. Appl. Polym. Sci. **2016**, *133*, 43125.

KEYWORDS: composites; foams; mechanical properties; nanoparticles; nanowires and nanocrystals; polyurethanes

Received 27 December 2014; accepted 4 November 2015

DOI: 10.1002/app.43125

INTRODUCTION

Polymer nanocomposites have attracted considerable attention in recent years as advanced new materials for modern technologies. This interest arises as a result of the improved properties of the polymer nanocomposites over that of the pristine polymer,[1] which resulted in design flexibility, lower life-cycle costs, and uniquely large applicability of the nanocomposites in various industrial fields. Polymer nanocomposites are advanced functional materials composed of nanoparticles dispersed within a polymeric matrix and forming a core–shell structure. As a result, the produced material combines the suitable properties of both components. Hybrid inorganic–organic nanocomposites such as polyurethane–silver nanocomposites (PU/AgNP) possess new chemical and physical properties that can be altered by the control of the synergistic association of the organic and inorganic components at nanoscale. Polyurethane polymers are produced by polycondensation polymerization of diisocyantes and long-chain polyols, in addition to a host of other chemicals used in order to control the desired specifications of the produced PU materials.[2] These materials are quite versatile and can be used in a variety of industrial applications such as rigid foams, flexible foams, adhesives, sealants, coatings, and thermoplastic elastomers. PU flexible foams can either be high-density or low-density foams. Bed mattresses and cushions are usually produced from PU foams with densities as low as 10–80 kg m^{-3} and comprises of open-cell cellular structures.[3]

Silver nanoparticles (AgNP) have ultrafine and uniform particle size distribution and possess unique electrical, optical, and biological properties.[4] In particular, they exhibit apparent antimicrobial behavior against different bacterial genre. The stability

and antibacterial activity of the nanoparticles are dependent on the surface chemistry of the silver nanofiller. For example, Kvitek *et al.*[5] reported stabilized nanosilver suspension to have better dispersion and antibacterial action. They also indicated that silver nanoparticles for antimicrobial or electronic applications are most effective when the particles contain minimum or no capping agents. Janardhanan *et al.*[6] synthesized silver nanoparticles from silver nitrate/glucose solution in the presence of an organic base with no external capping agents. They observed that the absence of glucose in the reaction produces silver oxide (Ag_2O) instead of metallic silver. The synthesized silver nanoparticles in this study possessed antibacterial activity against *Escherichia coli*. Silver ions and silver-based compounds are highly toxic to microorganisms showing strong biocidal effects on as many as 12 species of bacteria including *E. coli*, yeast, and *Staphylococcus aureus*.[7]

While the silver nanoparticles showed major antimicrobial activity against yeast and *E. coli*, their inhibitory effect on *S. aureus* growth was mild, which suggests that the antimicrobial effects of AgNP is specific against Gram-negative bacteria. The antimicrobial mechanism of silver was shown to depend on the presence of water and oxygen. Elemental silver particles are released in the form of silver ions which pass through the cell membrane and binds strongly to the electron releasing groups in the biological molecules in bacteria containing sulfur, oxygen, and/or nitrogen.[8–10] Some studies have reported that the positive charge on the Ag ion is crucial for its antimicrobial activity through the electrostatic attraction between negatively charged cell membrane of the microorganisms and the positively charged nanoparticles.[11–13]. Although silver salts and complexes are effective antimicrobial agents, their use may result in unwanted adsorption of ions in epidermis cells and sweat glands. The silver nanoparticles, on the other hand, show similar mechanism against bacteria but do not result in the side effects caused by silver salts. Zapata *et al.*[8] considered *in situ* polymerization as the most promising technique to produce polymer nanocomposites since it is based on the direct composite preparation in the presence of a nanofiller. For the *in situ* polymerization, the homogeneous dispersion of the nanoparticles in the polymer matrix was much improved and the compatibility between the inorganic silver nanoparticles and the polymer was greatly enhanced.

Polyurethane aging is an important process when considering long-term stability of industrial materials. Thermal degradation of polyurethanes is a kinetic process that is dependent on the chemical structure of the polymeric chains and the degradation temperature.[14] According to Chattopadhyay and Webster,[15] the thermal excitation induces complex vibration and rotation within the local space of the covalent bonds present in the polyurethane chains of the nanocomposites. With further excitation, these bonds can break to form a variety of fragment radicals or small molecules, which may recombine or undergo further fragmentation.[1,16–18] Ultimately, the resulting fragments may be vaporized, diffused out, or carbonized. The decomposition process ends with the loss of all volatile material and char formation (a complex insoluble material) that does not change further above the char temperature. Depending on the structure of the PU, char is composed of polynuclear aromatic carbon-containing compounds with heteroatoms such as oxygen, nitrogen, phosphorous, and sulfur. In addition to the carbonaceous (char) residue, inorganic residue might also be present and originates from the heteroatoms contained in the PU or from the incorporated inorganic nanoparticles.[19] The thermal stability is therefore a direct measure of molecular rigidity since the chemical degradation depends on macromolecular chain excitation and motion gained from the thermal energy during exposure to a high temperature.[20] In general, the thermal degradation of polyurethanes involves an initial stage where trapped volatile materials are released.

It is the purpose of this work to develop novel polyurethane flexible foams with induced antimicrobial characteristics for use in intensive care units and low-immunity patients' rooms, where disinfection and sterilization are crucial especially for immunocompromised patients. Silver nanoparticles will be used to induce the antimicrobial characteristics of the foam, which are also expected to result in the improvement of its mechanical performance. *In situ* polymerization of the urethane polymers in the presence of the silver nanoparticles will be used to prepare the resultant foams to ensure homogenous distribution of the silver nanoparticles within the polymeric matrix. The study will also focus on the characterization of the thermal, mechanical, and antimicrobial performance of the nanocomposites. The influences of the silver nanoparticles on the thermal degradation of the resultant foam and the molecular modeling of the surface interactions between the inorganic silver nanoparticles and the polyurethane chains are also investigated.

EXPERIMENTAL

Materials and Synthesis

All the polyurethane nanocomposite foams were prepared on location at the chemistry labs of Dow Mideast Systems SAE, a subsidiary of Dow Chemical Worldwide and using Dow's industrial systems and formulae for commercial flexible foam products to ensure that the results of this study can be applied directly into the manufacturing process. Dow's PU polyol blend and isocyanate prepolymer used in this study to produce the flexible foams were Voralux™ and Specflex™, respectively. The Voralux™ polyol blend had an OH value of 43 mg/g and contained the poly(ethylene glycol)-terminated polyether polyol, stannous octoate blowing catalyst, dibutyltindilaurate as a surfactant for flexible PU foaming and distilled water as the blowing agent. The Specflex™ prepolymer system had 30%part by weight NCO % content and contained polymeric diphenylmethanediisocyanate (MDI) with 2.7 NCO-functionality and average molecular weight of 340 g mol^{-1}. The powder silver nanoparticles (CAS-No.: 7440-22-4) used as the nanofiller in this study was supplied by Sigma-Aldrich Company and had the product number 576832. The silver particles had a purity of 99.5% and were coated with poly(vinylpyrrolidone) (PVP) to allow for good dispersion in the polar polyol blend by stabilizing the nanoparticles against agglomeration. The nanoparticles were 100 nm in diameter and had a surface area of 5.0 m^2/g. Various foam formulations with different AgNP loadings were produced: 0% AgNP (control sample), 0.1%AgNP, 0.5% AgNP,

and 1%AgNP. The mass of silver nanofiller corresponding to each formulation was mixed thoroughly with the polyol blend by a mechanical stirrer at a speed of 3000 rpm. The polyol blend incorporating the nanofiller was then allowed to react with the isocyanate prepolymer to produce *in situ* the AgNP-loaded nanocomposites with the desired filler loadings. The produced foams were all of a density around 32 kg m^{-3}, a typical density for commercial flexible foams.

Scanning Electron Microscopy (SEM)

The SEM used in the analysis was SUPRA 55 LEO SEM, a high-resolution FEGSEM for the analysis of materials and semiconductors and has the variable pressure option to examine non-conducting samples. The microscope has also an EDAX EBSD system for mapping the crystal orientation of materials.

Mechanical Properties Characterization

Influence of the incorporation of the silver nanoparticles of different loadings on the mechanical performance of the polyurethane flexible foams was characterized by a variety of crucial industry-standard tests such as follows.

Steel Ball Rebound Test. The steel ball rebound test (ASTM Designation: D3574-05) was performed on all the nanocomposite foams. A steel ball was left to drop 30 cm onto the surface of the samples and the rebound distance of the steel ball was measured. The test was repeated 12 times for each specimen to ensure a reliable average of the measured rebound distance. The test measures the resilience of the foam in relation to how much energy resulting from the impact of the steel ball with the surface of the foam has dissipated due to the presence of secondary interactions present within the polymer matrix such as the relaxation of the polymeric chains or formation and dissociation of hydrogen bonds.

Hardness. The hardness test performed is the indentation hardness test. Hardness measurements were performed using a standard type C durometer Model 307L, PTC Instruments, USA, in accordance with the standard test method for flexible properties (ISO 2439, ASTM designation: D3574-86). Five measurements of hardness at different positions of the various nanocomposite foams were made which were at least 3 cm apart and were averaged to generate the reported hardness values for each sample. All measurements were carried out at room temperature.

Compressive Strength Test. The various nanocomposite foam specimens of parallel flat faces having dimensions of 10 × 10 × 5 cm were held between two parallel plates and were subjected to a compression test (Designation: ASTM D3574). The force required to compress each sample at a continuous and constant rate was then measured to produce the corresponding load/extension curves. The compressive strength tests of the various foams were carried out at Dow Mideast Systems labs according to the industry standards.

Compression Set Test. The dry aged compression set test (ISO 1856;ASTM Designation: D3574) is a measure of the residual deformation of a foam specimen which has been subjected to a given fixed long-term deformation for a given time. Specimens of 5 × 5 × 2.5 cm dimensions were compressed between steel plates to 75% of their original thickness using spacers and stored for 22 h at 80°C. The specimens were then released and allowed to recover at room temperature for 30 min and their thickness was measured. The compression set is thus expressed as the percentage loss in thickness resulting from the degree of prolonged compressive strain applied on the specimen according to

$$C_t = [t_0 - t_f / t_0] \times 100\% \quad (1)$$

where C_t is the compression set expressed as a percentage of the original thickness, t_0 is the original thickness of the test specimen, and t_f is the final thickness of the test specimen.

Stress Relaxation Measurements. The stress relaxation isotherms of the various PU/AgNP foams at room temperature were obtained using step-compression stress relaxation technique. Specimens of 5 × 5 × 2.5 cm dimensions were held between two parallel plates with the lower one fixed in place and the upper one connected to a traveling strain gauge (Statham model G1-16-350). As the upper plate is allowed to move down, it compresses the foam sample. The samples were subjected to a stepwise compression by moving the upper plate down at fixed intervals. At each interval, the foam sample was allowed to relax till equilibrium. The main difference between testing the foam samples using this technique and the compressive strength technique is that the samples are allowed to relax here at various strain intervals and the corresponding stress values are measured at equilibrium permitting the stress–strain behavior of the nanocomposite foams to be evaluated using Mooney–Rivlin equation to explore possible deviation to the Gaussian behavior of the foams as a result of the incorporation of the silver nanoparticles into the foam composites. A constant voltage DC power supply (Hewlett Packard 6217) was used to supply approximately 14 V potential to the transducer and was connected to DS1M12 digital oscilloscope & Wave Form generator for output data recording. The transducer was frequently calibrated using a set of standard weights. Its output was found to remain constant over the usual time span of an experiment. Prior to placing the sample between the two plates, two thin lines were drawn on it by means of a marker. The exact length of the thus-demarcated section of the sample was measured precisely at the desired temperature by means of a cathetometer (Gaertner Scientific Corp., Model M940-303P, precision 1 micron), and the thickness and width of the foam cuboid were also determined in the same exact manner. Three measurements each along the thickness and width of the cuboid were taken and the average cross-sectional area, A^*, was determined. The upper clamp was raised to a position giving the desired elongation of the strip in a stepwise manner. The distance between the two lines was measured with a cathetometer and recorded as the length L. The ratio of L to L_0 (initial length) presents the compression (strain), α. The potential from the stress gauge was calibrated in terms of Newtons (N). The stress relaxation measurements were made using a sequence of increasing values of the compression as mentioned earlier. The values of the elastic force f were recorded at every strain step for the duration of the relaxation experiment. The equilibrium elastic force, f^*, was noted after the force reading has become sensibly constant for at least 15 min. The elastic quantity of interest for the stress–

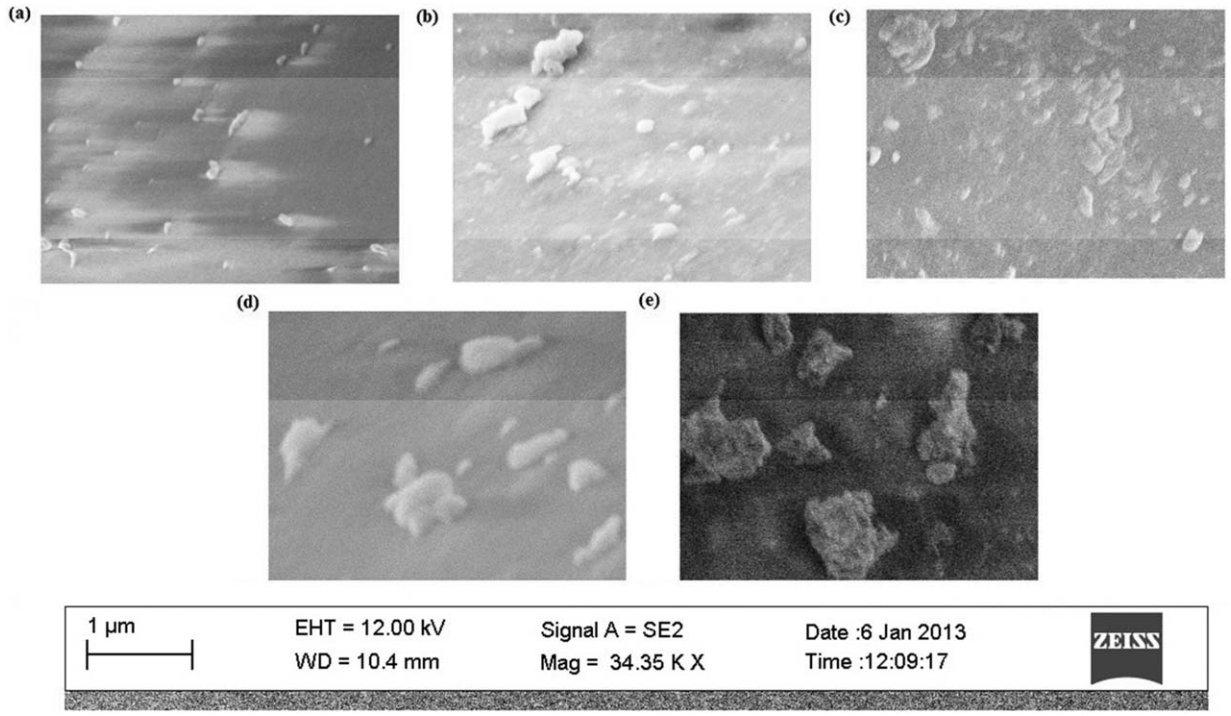

Figure 1. SEM micrographs of PU/AgNP nanocomposite foams.

strain investigation portion was the reduced stress, $[f^*]$, or modulus defined by[21–23]

$$[f^*] = f/[A^*(\alpha - \alpha^{-2})] \quad (2)$$

Accelerated Thermal Aging

The four PU/AgNP formulations of 0%, 0.1%, 0.5%, and 1% silver nanofiller were subjected to an accelerated thermal aging treatment using the oven method described in ASTM Designation D0573-99. Various foam specimens were placed in an air oven preheated at 140°C. The aging duration began at the time the specimens were placed in the oven and continued for time intervals of 3 and 10 days at 140°C. After aging, the specimen were removed from the oven, cooled to room temperature on a flat surface and allowed to stand for not less than 24 h prior to further processing. The aged specimens were all subjected to the same characterization methods described thus far.

Antimicrobial Performance Testing

In order to test the antimicrobial activity of the produced PU/AgNP nanocomposite foams, bacterial cells were cultured on both liquid and solid media. Antimicrobial activity was assessed by growth inhibition of both Gram-positive *Staphylococcus* sp., and two Gram-negative *Klebseilla* sp. and *E. coli* when the different foams were added to the cultures. Additionally, the silver concentration that would be the best in inhibiting the bacterial growth was assessed. In each bacterial liquid cultures, rectangular small pieces (around 1 × 1 cm) have been cut from each foam sample and immersed in 10 mL LB (Luria–Bertani) broth and incubated overnight at 37°C with continuous shaking. Bacteria's growth was measured by evaluating the optical density of each sample at 600 nm. On the other hand, LB agar plates were prepared and used to visualize the inhibition zone of the bacterial growth through adding a small piece of each sample on the plate after the streaking of the bacteria.

RESULTS AND DISCUSSION

Scanning Electron Microscopy (SEM)

SEM micrographs of the PU/AgNP nanocomposite foams are shown in Figure 1. The upper row of micrographs represents the variation in the AgNP loadings of (a) 0.1%, (b) 0.5%, and (c) 1% loadings. The lower row of micrographs represents the influence of the thermal degradation treatment on the silver nanoparticles in the nanocomposite foams of 0.1% loading subjected to (d) 3 and (e) 10 days durations. The two snapshots on the left side of the figure are the same and refer to the 0.1% sample at 0 days thermal treatment. They clearly indicate that the AgNP nanoparticles are uniformly distributed within the PU matrix without significant agglomeration or clustering. The increase in the AgNP loading from 0.1% to 0.5% and 1% loadings has apparently resulted in the agglomeration of the nanoparticles as could be shown in Figure 1(b,c). Strikingly, thermally treated 0.1% samples showed even more clustering than that resulted from the increase in the AgNP content, which indicates an apparent loss of the nanocharacteristics of the silver nanoparticles as they coalesce and agglomerate. These observations are quite significant and will have a major impact on the various thermodynamic, mechanical, and antimicrobial properties of the foam as will be discussed later.

Impact on the Resilience and Hardness of the PU/AgNP Nanocomposite Foams

One of the most widely used tests in foam characterization is the ball rebound test, which is an indication of the elasticity of the PU foam in relation to the foam resilience and the amount

Table I. Steel Ball Rebound Values for Various PU/AgNP Nanocomposites with Different AgNP Loadings at Different Intervals of Thermal Degradation

	Ball rebound at different aging intervals (cm)		
Loading AgNP (%)	0[a] days	3 days	10 days
0[b]	10	9	10
0.1	10.5	10	10
0.5	10.5	10	11
1.0	11	11	10

[a] 0 days in the oven refers to PU samples that were not subjected to any thermal aging treatment.
[b] 0% AgNp loading refers to pure PU samples without any nanofiller loading.

of energy dissipated as a result of the impact of a steel ball with the foam surface. Table I lists all the ball rebound values for the different AgNP-loaded nanocomposite foams in comparison to the pristine PU foam. The table indicates the apparent resilience of the foams even after being subjected to the thermal degradation treatment for long durations. It is obvious from the table that all the foams had similar ball rebound values at various AgNP loadings and different thermal degradation durations. This clearly confirms that the incorporation of the silver nanoparticles did not cause a loss in the foam elasticity. It also indicates that the thermal degradation treatment at the low temperature of 140°C well below the thermal decomposition temperature of the PU chains of 250°C did not influence the relaxation of the polymeric chains within the polymer matrix.

Another industry-standard characterization technique for PU foams is Shore C hardness.

It is a measure of the resistance of the cellular foam to indentation, scratching, or abrasion. Similarly, Table II lists the Shore C hardness values for the different foams at various durations of the thermal degradation treatment. As is the case with the ball rebound test, it is clear that both the incorporation of silver nanofiller into the polymeric matrix and subjecting the foams

Table II. Shore C Hardness Readings for Various PU/AgNP Nanocomposites with Different AgNP Loadings at Different Intervals of Thermal Degradation

	Hardness readings at different aging intervals		
Loading AgNP (%)	0[a] days	3 days	10 days
0[b]	26	27	27
0.1	30	31	29
0.5	30	30	29
1.0	31	31	30

[a] 0 days in the oven refers to PU samples that were not subjected to any thermal aging treatment.
[b] 0% AgNp loading refers to pure PU samples without any nanofiller loading.

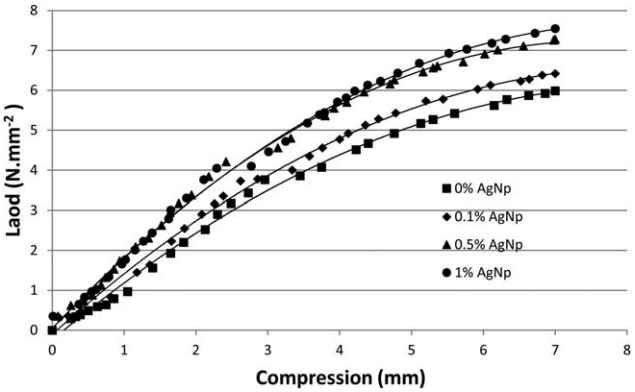

Figure 2. Compressive strength of the neat and various silver-nanocomposite PU foams with different nanofiller loadings not subjected to any thermal degradation treatment.

to a prolonged thermal degradation treatment did not influence the response of the different foams to the applied indentation force, a clear indication of no loss in the polymeric integrity in both cases.

Compressive Strength of the PU/AgNP Nanocomposite Foams

Figures 2–4 and Table III represent the compressive strength of the various loaded PU nanocomposite foams as a function of the nanofiller loading at different durations of 0, 3, and 10 days of the thermal degradation treatment, respectively. Figure 2 clearly shows that the increase in the nanofiller loading for non-thermally treated foams has increased the compressive strength of the PU foams due to the filler effect strengthen the polymeric chains and providing more resistance to the applied load. Figures 3 and 4, however, illustrate the influence of the thermal aging treatment on the compressive strength of the various PU foams. The figures, however, indicate that the increase in the aging durations has resulted in an apparent weakness of the different foams. Moreover, the compressive strength of the different foams has reached comparable values at 10 days thermal aging treatment indicating that higher nanofiller loadings have catalyzed the degradation kinetics of the polymeric chains especially those chains in close proximity to or adsorbed onto the surface of the filler nanoparticles. As these chains are degraded,

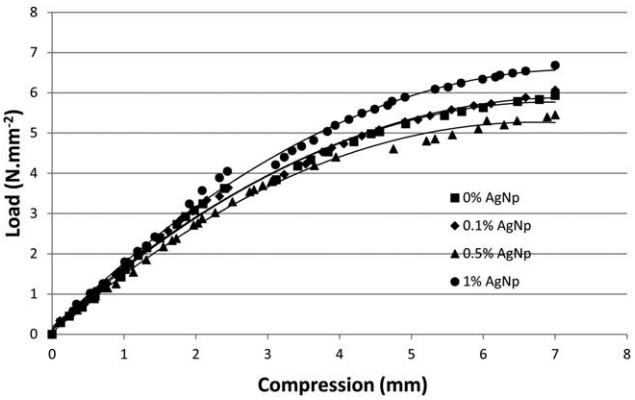

Figure 3. Compressive strength of the neat and various silver-nanocomposite PU foams with different nanofiller loadings subjected to 3 days thermal degradation treatment.

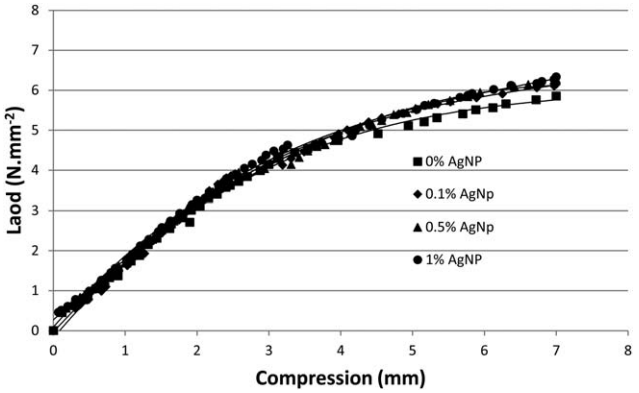

Figure 4. Compressive strength of the neat and various silver-nanocomposite PU foams with different nanofiller loadings subjected to 10 days thermal degradation treatment.

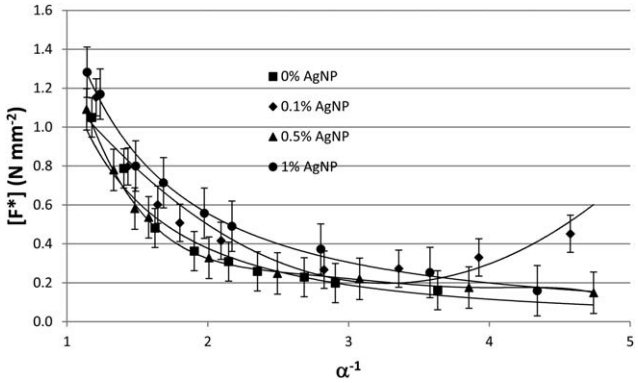

Figure 5. Mooney–Rivlin isotherms of the neat and various silver-nanocomposite PU foams with different nanofiller loadings not subjected to any thermal degradation treatment.

they no longer contribute to the overall strength of the polymeric materials causing the compressive strength of the various loaded PU nanocomposite foams to approach that of the pristine polymer. It could be also observed from the figures that for the pristine PU foam that the compressive strength of the foam has actually increased slightly with longer duration of the foam in the oven. This could be explained on the basis that in absence of any metallic nanofiller particles, there was obviously no catalytic influence on the thermal degradation kinetics. At the low oven temperature of 140°C well below the decomposition temperature of 250°C, the pristine polymer was subjected to slow annealing process which caused the PU chains to align next to each other in order to maximize their hydrogen bonding and consequently their overall strength. The figures also illustrate clearly the failure of the compressive strength of the PU foams at high loading of the nanofiller particles. It is possible in these cases that as the amount of the nanofiller increases, the nanoparticles agglomerate into macroscopic particles, which catalyzed the degradation kinetics and resulted in the observed failure of the compressive properties. It could be clearly observed that the greater the amount of the nanofiller, the greater the likelihood for the nanoparticles to seek out each other, coagulate and lose their nanocharacteristics as was confirmed by SEM.

Table III. Compression Set Percentages for Various PU/AgNP Nanocomposites with Different AgNP Loadings at Different Intervals of Thermal Degradation

	Compression set at different aging intervals (%)		
Loading AgNP (%)	0[a] days	3 days	10 days
0[b]	12	12	12
0.1	8	12	12
0.5	8	12	12
1.0	12	12	12

[a] 0 days in the oven refers to PU samples that were not subjected to any thermal aging treatment.
[b] 0% AgNp loading refers to pure PU samples without any nanofiller loading.

Stress Relaxation Measurements

Another way to characterize the influence of the incorporation of the silver nanofiller on the mechanical performance of the PU foams is through the evaluation of the equilibrium stress relaxation of the synthesized foams. The representation of the stress–strain data is based on the Mooney–Rivlin equation:

$$[f^*] = 2C_1 + 2C_2\alpha^{-1} \quad (3)$$

where $2C_1$ and $2C_2$ are constants.

Typical isotherms of this type are shown in Figures 5–7 for the AgNP-loaded PU nanocomposite foams as a function of the nanofiller loading at different durations of 0, 3, and 10 days of thermal degradation treatment, respectively. According to eq. (3), the reduced stress of the samples should decrease with an increase in the strain. Interestingly, for all the PU samples except for the 0.1% AgNP-loaded foam, this did occur following a Gaussian behavior. For the 0.1% AgNP-loaded foam, a Gaussian behavior was also observed up to high strain values. Instead of continuing to decrease, an upturn in the modulus values was observed. Even though it is quite normal for the pristine polymer to show the observed Gaussian behavior, it is rather surprising that while the 0.1% AgNP-loaded foam

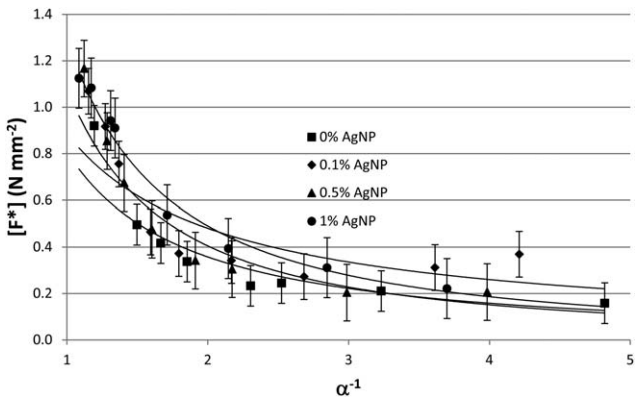

Figure 6. Mooney–Rivlin isotherms of the neat and various silver-nanocomposite PU foams with different nanofiller loadings subjected to 3 days thermal degradation treatment.

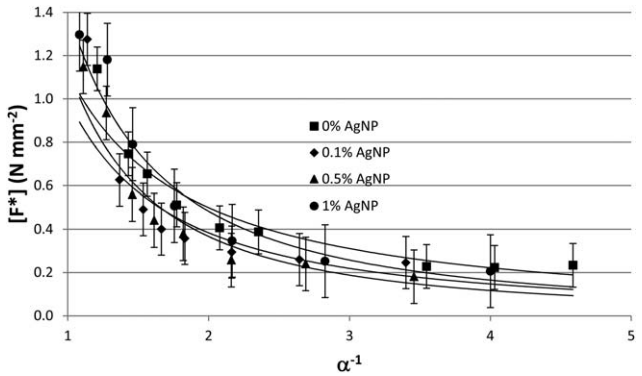

Figure 7. Mooney–Rivlin isotherms of the neat and various silver-nanocomposite PU foams with different nanofiller loadings subjected to 10 days thermal degradation treatment.

showed a non-Gaussian behavior, PU nanocomposite foams with higher AgNP loadings of 0.5% and 1% reversed back to a normal behavior. This non-Gaussian behavior is usually associated with either strain-induced crystallization or due to a filler effect. The interesting issue in this case is the disappearance of this non-Gaussian effect at both higher loadings of the silver nanoparticles and at longer durations of the thermal degradation treatment (Figures 6 and 7). This could only be explained through the coagulation of the nanofiller particles into macroscopic silver particles followed by the migration of these particles to the surface. In case of higher loading of the nanoparticles, it is quite easily for these particles to seek each other and coagulate. As the result of this coagulation and the small thickness of the PU strands in the open-cell foam structure, these particles have effortlessly migrated to the chain surface as confirmed by the SEM measurements, Figure 1. On the other hand, for even low AgNP loading, long durations of the thermal degradation process has also resulted in the coagulation of the silver nanoparticles as the annealing process instigated the PU chains to maximize their hydrogen bonding formation and thus allowing the silver nanoparticles to agglomerate and resulting in the diminishing of the observed non-Gaussian behavior. This can only be possible if the interfacial interactions between the filler particles and the polymeric chains are not strong enough at higher loadings of the nanofiller to stabilize the nanocomposite structure. To test the influence of the AgNP loading on the interfacial interactions between the filler particles and the polymeric chains, molecular modeling techniques of the nanocomposites have been performed.

Molecular Modeling of the Interfacial Interaction between the Nanofiller and the PU Chains

It is obvious from the previous discussion that the interfacial interaction between the polymer chain and the filler nanoparticles plays an important role in controlling the thermodynamic stability and the mechanical performance of the nanocomposites in direct relation to the conformational characteristics of the polyurethane chains. Molecular modeling techniques could be used to simulate the interfacial interactions between the PU chain and the silver nanofiller through the evaluation of the cohesive energies and the enthalpy of mixing the filler particles and the polymeric chains, ΔH_{mix}, according to[24]

$$\Delta H_{mix} = \phi_1 CED_1 + \phi_2 CED_2 - CED_{12} \quad (4)$$

where ϕ_i refers to the volume fraction of component i and CED_i refers to the cohesive energy density of system i, defined as the energy required to break all the intermolecular physical links in a unit volume of a material, and is given by

$$CED = \Delta E/V \quad (5)$$

which can be estimated readily from the simulation data by calculating the energy of the parent polymer chain in bulk with the periodic boundary conditions implemented, E_{bulk}, and the energy of isolated chain with the identical conformation in vacuum, E_{vac}, representing the chain in the gas phase:

$$CED = (E_{vac} - E_{bulk})/V \quad (6)$$

Molecular models of the PU/AgNP nanocomposites of different ratios were constructed and investigated using the Discovery module in Materials Studio® simulation package available from Accelyrs, Inc., UK.[25] Each simulated molecular cell contained one silver nanocluster of 20 Å radius. Different simulated cells containing an increasing number of the PU chains mixed with the silver nanocluster were simulated to investigate the influence of increasing the PU content on the enthalpy of mixing the nanofiller particle with the PU chains. Specifically, five cells were constructed and investigated containing 5, 10, 15, 20, and 25 PU chains. The modeled PU chain was represented as a hard block sequence of three consecutive MDI units separated by single ethylene glycol unit and terminated at both sides with 10-unit-long poly(ethylene glycol)-terminated poly(propylene glycol) segment representing the terminal ends of the soft segments. Figure 8 is a schematic representation of a simulated molecular cell of 20 PU chains mixed with the silver nanocluster. The periodic boundary condition were imposed to ensure that replicas of the

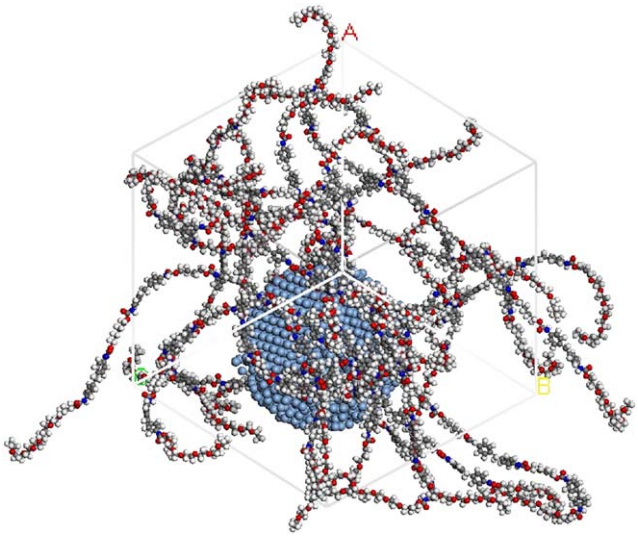

Figure 8. Graphical representation of a simulated molecular cell of PU chains mixed with silver nanoparticle of 20Å radius. The periodic boundary condition ensures that replicas of the nanoparticle are introduced in an infinite array of the neighbouring cells and are included in the estimation of the interfacial interactions between the polymer chains and the nanoparticles. [Color figure can be viewed in the online issue, which is available at wileyonlinelibrary.com.]

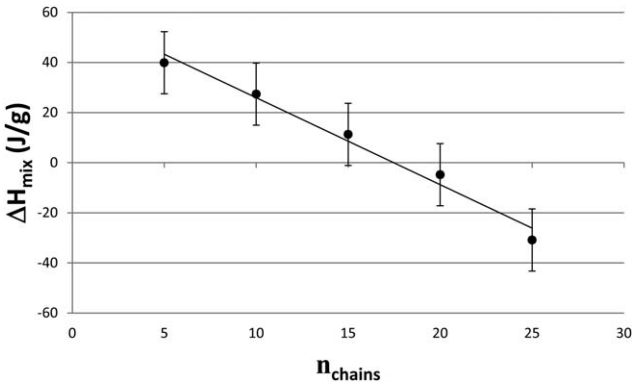

Figure 9. The dependence of the enthalpy of mixing the PU polymer chains with the silver nanoparticles at various volume fractions of the nanofiller.

nanoparticle is introduced in an infinite array of the neighboring cells and are included in the estimation of the interfacial interactions between the polymer chains and the nanoparticles. The cells were all simulated using COMPASS force field assigned charges and Ewald summation method. After the construction is complete, each simulation cell was minimized using the MS Discover module till complete convergence. Once the simulation cells were minimized, they were all subjected to annealing procedures involving five annealing cycles with initial temperature of 300 K and mid-cycle temperature of 500 K. Each annealing cycle had five heating ramps per cycle and ran for 1000 dynamics steps per ramp. The purpose of an annealing strategy is to attempt to find different local minimum energy structures by using the higher temperature periods of each annealing cycle to attempt to overcome energy barriers. Following the annealing procedures, molecular dynamics runs using NVT ensemble for 1 ns with 1 fs time step at the temperature of 298 K were performed to produce the desired trajectories for further molecular analysis. Full trajectories were saved every 100 steps. Four different runs were carried out for better averaging. Data calculated from eq. (4) are shown in Figure 9 as a function of the number of PU chains. It is clear from the figure that the smaller the PU content, the higher the values of the enthalpy of mixing. Positive values for the enthalpy of mixing indicate repulsive interactions between the nanoparticles and the polymeric chains at higher PU content implying a phase separation between the polymeric phase and the silver nanocluster. This is quite interesting since it confirms the conclusions made earlier that the increase in the silver nanoparticle content drives the phase separation and weakens the overall performance of the nanocomposite as the silver nanoparticles seek each other and coalesce due to the repulsive interactions between the PU chains and the silver nanoparticles. Once the silver nanoparticles start to agglomerate, they lose their nanocharacteristics with a negative impact on the performance of the nanocomposites. This is also in line with other experimental observation from neutron scattering results,[26,27] that the chains are forced to adopt more flattened and extended configurations resulting in a type of "strain amplifications." At higher loadings of the filler, the particles become less diluted by the matrix chains and the nanoscopic particles aggregate and interconnect forming a second network interpenetrating the polymer ("filler networking"), leading to the observed percolation behavior.[28,29]

Evaluation of the Antimicrobial Characteristics of PU/AgNP Nanocomposite Foams

The four different samples, 0%, 0.1%, 0.5%, and1% AgNP-loaded PU nanocomposite foams were tested for antimicrobial activity on Gram-positive (*Staphylococcus* sp.), and the Gram-negative *Klebseilla* sp. and *E. coli*. The study is also extended to examine the antimicrobial activities of the thermally degraded samples for 3 and 10 days. The antimicrobial property was tested on both liquid and solid media. In the presence of *E. coli*, a well-defined zone of inhibition was observed for the 0.1% AgNP-loaded sample that was not subjected to any thermal degradation treatment in contrast to the nonloaded (control) foam sample, which showed no inhibition zone. In liquid media (LB), cells were grown overnight and following the bacterial subculturing, the foams were added. After an overnight incubation, the optical densities were measured and the readings are shown in Table IV. For samples that were not subjected to thermal treatment, incubation of the 0.1% foam inhibited the growth of *Klebseilla* sp. and *E. coli* greatly and to some extent that of the *Staphylococcus* sp. For samples with higher AgNP loadings or samples subjected to thermal treatment of 3 and 10 days, there was no indication of growth inhibition. This is very interesting since these observations coincides fully with those of the SEM micrographs, which indicates that higher AgNP loading and/or exposure to long-term thermal treatment causes the nanoparticles to agglomerate into macroscopic particles and resulting in a loss of their nanocharacteristics, reduction of its surface area, and consequently lowering its effectiveness as an antimicrobial agent.

It should be noted however, that despite the many advantages of AgNP, their leaching or migration to the surface of the foam may have potential toxicity if it was allowed to get in contact with the human skin. However, it should be noted here that PU foams are cross-linked polymers with both intricate networks of hydrogen bonding and complex phase separation on the molecular level. On the macroscopic level, cellular foams provide even more barriers to the migration of any additives throughout the foam structure. It is thus expected that leaching or migration of the nanoparticles is close to none when they are well embedded within the PU matrix during their *in situ* polymerization. Nonetheless, further investigation on this particular point is certainly needed to confirm this prospect and could be the topic of a subsequent investigation.

Table IV. Optical Density of the Various Microbial Subcultures with the Nanocomposite Foams of Different AgNP-Loadings as an Indication of the Antimicrobial Efficiency of the Various Foams

	Optical density		
Loading AgNP	*Klebseilla* sp.	*Staphylococcus* sp.	*E. coli*
0[a]	0.949	0.169	0.007
0.1	0.184	0.131	0
0.5	0.835	0.146	0.006
1.0	0.95	0.176	0.01

[a] 0% AgNP loading refers to pure PU samples without any nanofiller loading.

CONCLUSION

Silver nanoparticle-reinforced thermoplastic polyurethane (PU/AgNP) nanocomposite foams prepared using *in situ* polymerization techniques in accordance with DOW chemicals' industrial standards exhibited antimicrobial properties, improved mechanical performance, and intact degradation profile, which may be potentially used in reverse precaution medical applications. Scanning electron microscopy indicated a homogeneous dispersion of the silver nanoparticle within the polymeric matrix at low filler loadings versus cluster formation at higher loadings. Step-compression stress relaxation of the nanocomposites showed optimum performance and lowest hysteresis for the 0.1% AgNP nanocomposites due to the confinement of the PU chains between the large number of the nanofiller particles. Main properties that characterize polyurethane foams such as resilience, hardness, and compression set were unaltered by the presence of the nanofiller. The presence of the nanoparticles did not affect the mechanical performance of the foams after the samples subjected to prolonged thermal degradation treatment indicating an intact thermal stability of these foams. SEM investigations indicated that the higher the loading of the nanoparticles or the longer the durations of the thermal degradation treatment, the higher the chance of these nanofiller particles to agglomerate and lose their characteristic nanoscopic nature. Molecular modeling confirmed the SEM observations that the higher AgNP content, the higher the repulsive interactions between the polymer chains and the silver nanoparticles, which caused the nanoparticles to seek each other out and coalesce into macroscopic particles. Incubation with 0.1% foam inhibited the growth of *Klebseilla* sp. and *E. coli* and to some extent that of the *Staphylococcus* sp. This is quite interesting since the 0.1% AgNP-loaded PU nanocomposite foam produced the best mechanical performance, which confirms that the remarkable nanoscopic distribution of low nanofiller loadings within the polymeric matrix induced by the *in situ* polymerization is the drive for the optimum mechanical and antimicrobial performance of the nanocomposite foams.

ACKNOWLEDGMENTS

The authors would like to acknowledge the support they received from Dow Mideast Systems SAE, a subsidiary of Dow Chemical Worldwide in providing the chemicals, flexible foam formulae and necessary equipment required to synthesize and test the various antimicrobial foams in accordance with the well-established industrial standards for foam manufacturing.

REFERENCES

1. Madkour, T. M.; Hagag, F. M.; Mamdouh, W.; Azzam, R. A. *Polymer* **2012**, *53*, 5788.
2. Madkour, T. M.; Azzam, R. A. *J. Polym. Sci. Part A: Polym. Chem.* **2002**, *40*, 2526.
3. Saint-Michel, F.; Chazeau, L.; Cavaillé, J. Y. *Compos. Sci. Technol.* **2006**, *66*, 2709.
4. Andersen, P. C.; Jacobson, M. L.; Rowlen, K. L. *J. Phys. Chem. B* **2004**, *108*, 2148.
5. Kvitek, L.; Panacek, A.; Prucek, R.; Soukupova, J.; Vanickova, M.; Kolar, M.; Zboril, R. *J. Phys. Conf. Series* **2011**, *304*, 012029.
6. Janardhanan, R.; Karuppaiah, M.; Hebalkar, N.; Rao, T. N. *Polyhedron* **2009**, *28*, 2522.
7. Dror-Ehre, A.; Mamane, H.; Belenkova, T.; Markovich, G.; Adin, A. *J. Colloid Interf. Sci.* **2009**, *339*, 521.
8. Zapata, P. A.; Tamayo, L.; Páez, M.; Cerda, E.; Azócar, I.; Rabagliati, F. M. *Eur. Polym. J.* **2011**, *47*, 1541.
9. Kumar, R.; Münstedt, H. *Biomaterials* **2005**, *26*, 2081.
10. Jeong, S. H.; Hwang, Y. H.; Yi, S. C. *J. Mater. Sci.* **2005**, *40*, 5413.
11. Huang, H.; Yang, Y. *Compos. Sci. Technol.* **2008**, *68*, 2948.
12. Dibrov, P.; Dzioba, J.; Gosink, K. K.; Hase, C. C. *Antimicrob. Agents Chemother.* **2002**, *46*, 2668.
13. Sondi, I.; Salopek-Sondi, B. *J. Colloid Interf. Sci.* **2004**, *275*, 177.
14. Khatua, B. B.; Das, C. K. *Polym. Degrad. Stab.* **2000**, *69*, 381.
15. Chattopadhyay, D. K.; Webster, D. C. *Progr. Polym. Sci.* **2009**, *34*, 1068.
16. Dong, Z.; Li, Y.; Zou, Q. *Appl. Surf. Sci.* **2009**, *255*, 6087.
17. Kuan, H. C.; Ma, C. C. M.; Chang, W. P.; Yuen, S. M.; Wu, H. H.; Lee, T. M. *Compos. Sci. Technol.* **2005**, *65*, 1703.
18. Cai, D.; Jin, J.; Yusoh, K.; Rafiq, R.; Song, M. *Compos. Sci. Technol.* **2012**, *72*, 702.
19. Oprea, S. *Polym. Degrad. Stab.* **2002**, *75*, 9.
20. Pashaei, S.; Siddaramaiah, S. A. A. *J. Macromol. Sci. Part A* **2010**, *47*, 777.
21. Madkour, T. M.; Mark, J. E. *Macromol. Rep.* **1994**, *A31(SUPPLS 12)*, 153.
22. Madkour, T. M.; Hamdi, M. S. J. *Appl. Polym. Sci.* **1996**, *61*, 1239.
23. Chang, Y. W.; Kim, S.; Kang, S. C.; Bae, S. Y.; Korean, J. *Chem. Eng.* **2011**, *28*, 1779.
24. Madkour, T. M.; Salem, S. A.; Miller, S. A. *Phys. Chem. Chem. Phys.* **2013**, *15*, 5982.
25. Bicerano, J. Prediction of Polymer Properties; Marcel Dekker: New York, **2002**.
26. Nakatani, A. I.; Chen, W.; Schmidt, R. G.; Gordon, G. V.; Han, C. C. *Polymer* **2001**, *42*, 3713.
27. Nakatani, A. I.; Chen, W.; Schmidt, R. G.; Gordon, G. V.; Han, C. C. *Int. J. Thermophys.* **2002**, *23*, 199.
28. Witten, T. A.; Rubinstein, M.; Colby, R. H. *J. Phys. II* **1993**, *3*, 367.
29. Guan, L.; Jiménez, M. E. G.; Walowski, C.; Boushehri, A.; Prausnitz, J. M.; Radke, C. J. *J. Appl. Polym. Sci.* **2011**, *122*, 1457.